Quantum spin fluctuations and ellipticity for a triangular-lattice antiferromagnet

Randy S. Fishman

Materials Science and Technology Division, Oak Ridge National Laboratory, Oak Ridge, Tennessee 37831, USA

The effects of quantum spin fluctuations are investigated for the three-sublattice spin configurations of a geometrically frustrated triangular-lattice antiferromagnet in a magnetic field with easy-axis anisotropy. Because quantum fluctuations reduce the tilt of the spins toward the easy axis, the predicted distortion of the noncollinear state at zero field is too small to explain the ellipticity reported for the multiferroic state of $CuCrO_2$. Due to the change in spin angles, quantum fluctuations shift the boundaries between the collinear and noncollinear phases and open a gap in field between the two types of noncollinear phases.

It is well known that quantum fluctuations (QFs) significantly affect the spin states of a Heisenberg antiferromagnet (AF).[1] For many two-dimensional systems,[2] QFs lower the transition temperature to zero. Because an AF state is not an eigenstate of the Heisenberg Hamiltonian, QFs suppress the spin amplitudes of an AF even at zero temperature. QFs also alter the excitation energies about an AF ground state. In particular, several groups[3] have studied the change in excitation energies for a spin $S = \frac{1}{2}$ triangular-lattice AF, which has a classical $120°$ ground state with three equivalent sublattices.

Less understood are the effects of QFs on noncollinear spin states with inequivalent sublattices. The possible importance of QFs for such systems is demonstrated by the elliptical spin states observed in the multiferroic phases of $MnWO_4$,[4] $TbMnO_3$,[5,6] $CuFeO_2$,[7,8] and $CuCrO_2$.[9,10] If the generalized spiral $\langle \mathbf{S}_i \rangle = M_i (0, \sin\theta_i, \cos\theta_i)$ has an ellipticity $p \leqslant 1$, then the magnetic structure factor perpendicular to the easy axis is p times smaller than the magnetic structure factor parallel to the easy axis. In order of increasing p, $TbMnO_3$ ($S = 2$), $CuCrO_2$ ($S = \frac{3}{2}$), $MnWO_4$ ($S = \frac{5}{2}$), and $CuFeO_2$ ($S = \frac{5}{2}$) have ellipticities of 0.72, 0.79, 0.82, and 0.9, respectively. QFs play two important roles in altering the noncollinear states of these materials: suppressing the spin amplitude $M_i = S - \Delta M_i$ by ΔM_i and rotating the spin angle θ_i by $\Delta \theta_i$. We find that both quantum effects contribute to the ellipticity of a spiral spin state.

Because the noncollinear states of $TbMnO_3$, $CuFeO_2$, and $MnWO_4$ are incommensurate, evaluating the effects of QFs for those materials would be quite challenging. In order to qualitatively understand the effect of QFs on a noncollinear state with inequivalent sublattices, we examine the simple three-sublattice spin configurations of a geometrically frustrated triangular-lattice AF. Since the hexagonal layers of $CuCrO_2$ are only weakly coupled,[9,10] this model should describe the multiferroic state of $CuCrO_2$.[11] Another reason to focus on $CuCrO_2$ is that QFs are expected to play a more important role due to the moderate $S = \frac{3}{2}$ spins.

The geometry of a triangular-lattice AF is sketched in Fig. 1(a), with nearest-neighbor interaction $J_1 < 0$ and second- and third-neighbor interactions J_2 and J_3. The Hamiltonian of a triangular-lattice AF in a magnetic field H in the **z** direction can be written

$$\mathcal{H} = -\frac{1}{2} \sum_{i \neq j} J_{ij} \mathbf{S}_i \cdot \mathbf{S}_j - D \sum_i S_{iz}^2 - 2\mu_B H \sum_i S_{iz}. \quad (1)$$

Easy-axis anisotropy D favors collinear states with spins aligned along the z axis and may be experimentally controlled in materials like $CuFeO_2$ ($S = \frac{5}{2}$) by doping[8] or oxygen nonstoichiometry.[12]

For classical spins with large anisotropy (i.e., Ising spins), the four-sublattice collinear state $\uparrow\uparrow\downarrow\downarrow$ is stable in zero field for the range of parameters $J_1 < 0$, $-0.5|J_1| < J_2 < 0$, and $J_3 < J_2/2$.[13] As the anisotropy decreases, the $\uparrow\uparrow\downarrow\downarrow$ phase transforms into one of two possible noncollinear states (depending on the exchange parameters): either a distorted spiral with incommensurate wave vector or the three-sublattice phase sketched in the lower left of the phase diagram of Fig. 1(b).[14] While the former case corresponds to the multiferroic phase of Ga- or Al-doped $CuFeO_2$,[8] the latter case corresponds to the multiferroic phase of pure $CuCrO_2$.[11] With increasing field, the three-sublattice phase continuously transforms into the collinear $\uparrow\uparrow\downarrow$ phase at $H_c^{(1)}$ and then into another noncollinear three-sublattice phase at $H_c^{(2)}$.

To qualitatively understand the effects of QFs, we study the transition from the collinear $\uparrow\uparrow\downarrow$ phase into the two types of noncollinear three-sublattice phases. For the parameters used in Fig. 1(b), which are believed to describe $CuCrO_2$,[11] these noncollinear phases are stable at $D = 0$ on either side of the field $H_c^{(1)} = H_c^{(2)} = H_c \equiv 1.6S|J_1|/\mu_B$. Whereas the low-field phase below $H_c^{(1)}$ is characterized by a single independent angle $\theta_1 = -\theta_2$ ($\theta_3 = \pi$), the high-field phase above $H_c^{(2)}$ is characterized by two independent angles $\theta_1 = \theta_2$ and θ_3. These three-sublattice phases were first predicted[15] for a triangular-lattice AF with only nearest-neighbor interactions ($J_2 = J_3 = 0$). The low-field phase is chiral but the high-field phase is not.

Upon transforming the spins in their rotated reference frames to boson operators $a_\mathbf{k}^{(r)}$ and $a_\mathbf{k}^{(r)\dagger}$ (sublattices $r = 1$, 2, or 3),[1] the Hamiltonian can be expanded about the classical limit in powers of $1/\sqrt{S}$:

$$\mathcal{H} = S^2 E_0 + \mathcal{H}_{\text{int}} + SR_2 + \vartheta(S^0), \quad (2)$$

$$\mathcal{H}_{\text{int}} = S \sum_\mathbf{k} \mathbf{u}(\mathbf{k})^\dagger \cdot \underline{L}(\mathbf{k}) \cdot \mathbf{u}(\mathbf{k}), \quad (3)$$

where $\mathbf{u}(\mathbf{k}) = (a_\mathbf{k}^{(1)}, a_\mathbf{k}^{(2)}, a_\mathbf{k}^{(3)}, a_{-\mathbf{k}}^{(1)\dagger}, a_{-\mathbf{k}}^{(2)\dagger}, a_{-\mathbf{k}}^{(3)\dagger})$ is a six-component vector and $\underline{L}(\mathbf{k})$ is a 6×6 Hermitian matrix. The function $R_2(\theta_i)$ appears after the Hamiltonian is symmetrized in terms of the boson operators.[16] The term of order $S^{3/2}$, linear in the boson operators, vanishes when the classical
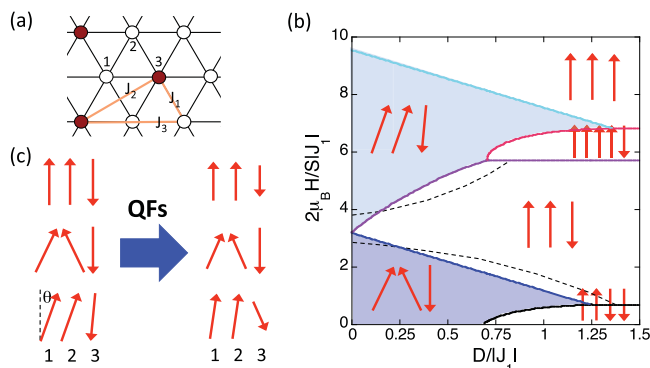
FIG. 1. (Color online) (a) The collinear three-sublattice state with up (white) and down (dark) spins on a triangular lattice with AF interactions J_1, J_2, and J_3. (b) The magnetic phase diagram for $J_2/|J_1| = -0.11$ and $J_3/|J_1| = -0.06$ with spin states of each phase indicated and the noncollinear phases shaded.[11] Qualitatively, the dashed curves are the phase boundaries shifted by QFs. (c) The qualitative effect of QFs on the collinear and noncollinear three-sublattice states.

energy $E_0(\theta_i)$ is minimized as a function of the spin angles θ_i. Each term in this expansion is a function of the normalized field $2\mu_B H/S$, which should be considered of order S^0.

Because the Boson operators $a_{\mathbf{k}}^{(r)}$ satisfy the commutation relations $[a_{\mathbf{k}}^{(r)}, a_{\mathbf{k'}}^{(s)\dagger}] = \delta_{\mathbf{k,k'}}\delta_{rs}$, $\mathbf{u}(\mathbf{k})$ satisfies the matrix commutation relation $[\mathbf{u}(\mathbf{k}), \mathbf{u}(\mathbf{k'})^\dagger] = \underline{N}\delta_{\mathbf{k,k'}}$, where $\underline{N}$ is the 6×6 matrix

$$\underline{N} = \begin{pmatrix} \underline{I} & 0 \\ 0 & -\underline{I} \end{pmatrix} \tag{4}$$

and $\underline{I}$ is the three-dimensional unit matrix. The interaction term $\mathcal{H}_{\text{int}}$ can be diagonalized by the transformation $\mathbf{u}(\mathbf{k}) = \underline{X}^{-1} \cdot \mathbf{w}(\mathbf{k})$, where $\underline{X}$ is a 6×6 nonunitary matrix satisfying $\underline{X}\underline{N}\underline{X}^\dagger = \underline{N}$. The vector $\mathbf{w}(\mathbf{k}) = (\alpha_{\mathbf{k}}^{(1)}, \alpha_{\mathbf{k}}^{(2)}, \alpha_{\mathbf{k}}^{(3)}, \alpha_{-\mathbf{k}}^{(1)\dagger}, \alpha_{-\mathbf{k}}^{(2)\dagger}, \alpha_{-\mathbf{k}}^{(3)\dagger})$ is defined in terms of Boson operators $\alpha_{\mathbf{k}}^{(r)}$ that also satisfy the commutation relations $[\alpha_{\mathbf{k}}^{(r)}, \alpha_{\mathbf{k'}}^{(s)\dagger}] = \delta_{\mathbf{k,k'}}\delta_{rs}$. Consequently, $\mathbf{w}(\mathbf{k})$ also satisfies the matrix commutation relation $[\mathbf{w}(\mathbf{k}), \mathbf{w}(\mathbf{k'})^\dagger] = \underline{N}\delta_{\mathbf{k,k'}}$.

Diagonalizing $\mathcal{H}_{\text{int}}$ yields

$$\mathcal{H}_{\text{int}} = S \sum_{\mathbf{k}} \mathbf{w}(\mathbf{k})^\dagger \cdot \underline{L}'(\mathbf{k}) \cdot \mathbf{w}(\mathbf{k}), \tag{5}$$

where $SL'(\mathbf{k})_{ij} = SL'(\mathbf{k})_{ii}\delta_{ij}$ has diagonal matrix elements $\{\epsilon_1(\mathbf{k}), \epsilon_2(\mathbf{k}), \epsilon_3(\mathbf{k}), \epsilon_1(\mathbf{k}), \epsilon_2(\mathbf{k}), \epsilon_3(\mathbf{k})\}/2$. Hence, we obtain the familiar expression

$$\mathcal{H}_{\text{int}} = \sum_{\mathbf{k},r} \epsilon_r(\mathbf{k})\left(\alpha_{\mathbf{k}}^{(r)\dagger}\alpha_{\mathbf{k}}^{(r)} + \frac{1}{2}\right), \tag{6}$$

with three branches of spin-wave energies $\epsilon_r(\mathbf{k})$. The energy $E = \langle \mathcal{H} \rangle$ can be written $E = S^2 E_0 + S E_2$ with order-S term $SE_2 = \sum_{\mathbf{k},r} \epsilon_r(\mathbf{k})/2 + SR_2$.

In the collinear $\uparrow\uparrow\downarrow$ phase for $D > D_c$, the anisotropy energy produces a gap in the spin-wave spectrum, but in the noncollinear phases below D_c, continuous rotational symmetry around the z axis generates a gapless Goldstone mode. As $D \to D_c^+$, the spin-wave gap vanishes at the ordering

wave vector $\mathbf{Q} = (4\pi/3)\mathbf{x}$ of the noncollinear three-sublattice phases.

The spin amplitude for sublattice r is given by $M_r = S - \Delta M_r$, where

$$\Delta M_r = \frac{3}{N} \sum_{\mathbf{k}} \langle a_{\mathbf{k}}^{(r)\dagger} a_{\mathbf{k}}^{(r)} \rangle = \frac{3}{N} \sum_{\mathbf{k},s} |X_{rs}^{-1}|^2. \tag{7}$$

The changes $\Delta\theta_i$ in the spin angles are evaluated by minimizing the total energy $E(\theta_i)$ as a function of the angles θ_i. With the expansions $\theta_i = \theta_i^{(0)} + \Delta\theta_i$, $\theta_i^{(0)}$ minimize the classical energy $E_0(\theta_i)$ and $\Delta\theta_i$ are of order $1/S$. It is straightforward to show that

$$\Delta\theta_r = -\frac{1}{SN} \sum_s Y_{rs}^{-1} \frac{\partial E_2}{\partial \theta_s}, \tag{8}$$

with the Hessian $Y_{rs} = \partial^2(E_0/N)/\partial\theta_r \partial\theta_s$ evaluated at the classical angles $\theta_i^{(0)}$.

Results for zero field with angles $\{\theta_1, \theta_2 = -\theta_1, \theta_3 = \pi\}$ are plotted in Fig. 2. The classical 120° phase with $\theta_1 = \pi/3$ is recovered as $D \to 0$. In this limit, the amplitudes of all three spins are suppressed by the same amount $\Delta M_r \approx 0.381$. With increasing D, spins 1 and 2 bend toward the z axis
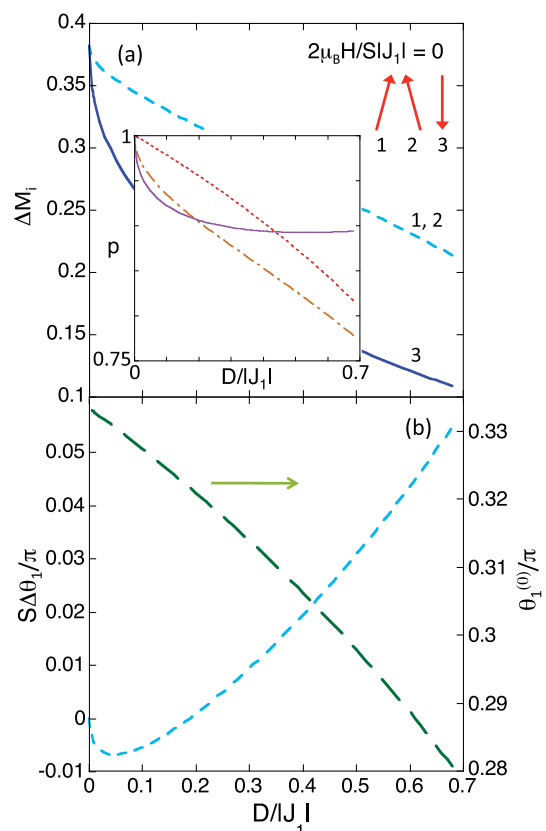

FIG. 2. (Color online) In zero field, (a) the suppression ΔM_i of the spin amplitudes, (b) the classical angle $\theta_1^{(0)}/\pi$ for site 1 and the change in angle $S\Delta\theta_1/\pi$ versus $D/|J_1|$. Recall that $\theta_2^{(0)} = -\theta_1^{(0)}$, $\theta_3^{(0)} = \pi$, $\Delta\theta_2 = -\Delta\theta_1$, and $\Delta\theta_3 = 0$. Inset in (a) is the ellipticity p of the $S = \frac{3}{2}$ noncollinear phase, for classical spins without QFs (short dashed) or for quantum spins, either including (solid) or not including (dash-dot) the change in the angles θ_1 and θ_2. Other parameters are as in Fig. 1(b).

and $\Delta M_1 = \Delta M_2$ exceeds ΔM_3. Hence, QFs produce an elliptical spiral state with maximal spin along the anisotropy axis. Qualitatively similar results were obtained in Ref. 17 to explain the elliptical spiral of TbMnO$_3$.[5,6]

The change $\Delta\theta_1 = -\Delta\theta_2$ in the spin angles due to QFs is plotted in Fig. 2(b). For large D, $\Delta\theta_1 > 0$, corresponding to a rotation away from **z**, but for $D/|J_1| < 0.19$, $\Delta\theta_1$ changes sign and spins 1 and 2 cant toward **z**. As $D \to 0$, the effect of QFs on the spin angles disappears and the 120° phase is restored.

With the magnetic structure factor defined by

$$F^\gamma(\mathbf{Q}) = \frac{1}{N}\sum_i \langle S_{i\gamma}\rangle \exp(i\mathbf{Q}\cdot\mathbf{R}_i), \qquad (9)$$

the ellipticity is given by $p = |F^y(\mathbf{Q})|/|F^z(\mathbf{Q})|$. For the three-sublattice noncollinear phase in zero field, $p = M_1\sqrt{3}\sin\theta_1/(M_3 + M_1\cos\theta_1)$. Even for classical spins without QFs, $p = \sqrt{3}\sin\theta_1/(1 + \cos\theta_1) < 1$ when $D > 0$ because spins 1 and 2 tilt toward the easy axis ($\theta_1 < \pi/3$).

The inset to Fig. 2(a) plots the ellipticities for classical spins (dash) and for quantum $S = \frac{3}{2}$ spins, either with (solid) or without (dash-dot) considering the effect of QFs on the angles. As expected, $p \to 1$ as $D/|J_1| \to 0$ for each case. For $D/|J_1| > 0.19$, p is substantially increased by the effect of QFs on the spin angles because $\Delta\theta_1 > 0$ and the tilt of spins 1 and 2 toward the easy axis is reduced. For $D = 0.68|J_1|$, which is the critical value for the transition from the noncollinear phase to the ↑↑↓↓ phase, the ellipticity without considering the effect of QFs on the angles is 0.778 while the corrected ellipticity is 0.894, larger even than the classical value of 0.817. So for large anisotropy, QFs actually enhance p above that for a classical spiral. The results of Ref. 17, which did not consider the effect of QFs on the spin angles, are in qualitative agreement with the dashed and dash-dotted curves.

For $H > H_c$, the noncollinear phase has two independent angles with configuration $\{\theta_1, \theta_2 = \theta_1, \theta_3\}$. When $2\mu_B H/S|J_1| = 4$, the second-order ↑↑↓ to noncollinear transition occurs at $D_c/|J_1| = 0.167$, as shown in Fig. 3. This transition becomes first order when $2\mu_B H/S > 5.07|J_1|$. Figure 3(a) indicates that QFs suppress the down spin more than the two up spins. In the collinear ↑↑↓ phase, $\Delta M_1 = \Delta M_2 = \Delta M_3/2$, which implies that the average spin $M_{av} = 1/3$ is not affected by QFs.[18] In the noncollinear phase, the down spin is even more suppressed compared to the up spins, and $\Delta M_3 - 2\Delta M_1 > 0$ grows with decreasing D.

The effect of QFs on the angles θ_i is shown in Fig. 3(b). Both $\Delta\theta_1$ and $\Delta\theta_2$ diverge at the critical value D_c, which implies that D_c is shifted from its classical value. By expanding $D_c = D_c^{(0)} + \Delta D_c$, the condition for the angles θ_i to approach their collinear values is

$$\theta_i^{(0)}\big(D_c^{(0)} + \Delta D_c\big) + \Delta\theta_i\big(D_c^{(0)-}\big) = \theta_i^{(0)}\big(D_c^{(0)}\big) \qquad (10)$$

or

$$\Delta D_c = -\frac{\Delta\theta_i}{\partial\theta_i^{(0)}/\partial D}\bigg|_{D_c^{(0)-}}, \qquad (11)$$

which is of order $1/S$. For the high-field noncollinear phase, the condition with either $\Delta\theta_1$ or $\Delta\theta_3$ yields the same result for
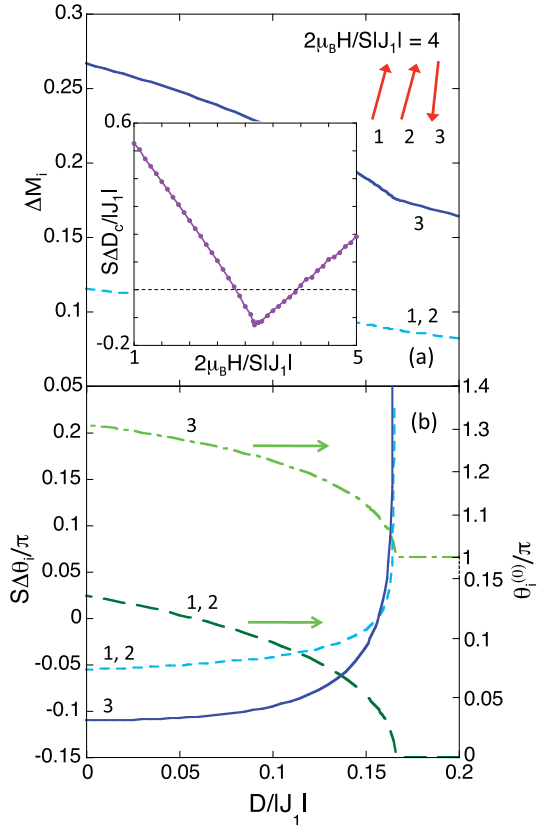

FIG. 3. (Color online) With $2\mu_B H/S|J_1| = 4$, (a) the suppression ΔM_i of the spin amplitudes and (b) the classical angles $\theta_i^{(0)}/\pi$ for each site and the change in angles $S\Delta\theta_i/\pi$ versus $D/|J_1|$. Other parameters are as in Fig. 1(b). Inset in (a) is the change in critical anisotropy $S\Delta D_c$ versus field.

ΔD_c, but for the low-field noncollinear phase, only $\Delta\theta_1$ can be used to evaluate ΔD_c.

Results for ΔD_c are plotted versus field in the inset to Fig. 3(a). We find that ΔD_c is a nearly linear function of field on either side of $2\mu_B H_c/S = 3.2|J_1|$, which separates the two types of noncollinear phases. Since $\Delta D_c < 0$ close to H_c, QFs open a gap in the phase diagram, as shown qualitatively in Fig. 1(b). Notice that this gap is asymmetric: wider above H_c than below. Of course, the actual size of the gap depends on the spin S. The opening of a magnetization plateau with $M_{av} = \frac{1}{3}$ due to QFs was first predicted by Chubukov and Golosov[19] for a triangular-lattice AF with $J_2 = J_3 = 0$ and $D = 0$.

For $2\mu_B H/S > 5.07|J_1|$, the transition from the collinear ↑↑↓ phase into the noncollinear phase is first order. Consequently, the condition for ΔD_c requires the order-S^0 energy $E_4(\theta_i)$, which attains different values on either side of the classical transition at $D_c^{(0)}$. That calculation is beyond the scope of this paper.

Qualitatively, the effects of QFs on the spin states are sketched in Fig. 1(c). In zero field, QFs generate an elliptical state with the smallest amplitude away from the anisotropy axis. At high fields, QFs act predominantly to suppress the down-spin amplitude.

This work was motivated by the elliptical spin states observed in multiferroic MnWO$_4$ ($p \approx 0.82$),[4] TbMnO$_3$

($p \approx 0.72$),[5,6] CuFeO$_2$ ($p \approx 0.9$),[7,8] and CuCrO$_2$ ($p \approx 0.79$)[9,10] in zero field. If the ferromagnetic moment of each hexagonal layer vanishes, then $2M_1 \cos\theta_1 - M_3 = 0$ so that $p = 0.79$ corresponds to $\theta_1 = 0.30\pi$ and $M_1/M_3 = 0.85$.

Using the easy-axis anisotropy $D/|J_1| \approx 0.17$[10] estimated for CuCrO$_2$, the classical value of p for the triangular-lattice AF is 0.913 while the quantum value is 0.910. Of course, the effect of QFs will be reduced compared to the predictions of this paper for three-dimensional CuCrO$_2$ with its weakly coupled planes. QFs will also be suppressed by easy-plane anisotropy, which generates a small spin-wave gap[9,10] in CuCrO$_2$. We conclude that the small ellipticity $p \approx 0.79$ of CuCrO$_2$ cannot be explained by QFs. One possible explanation for the pronounced ellipticities of CuCrO$_2$ and other materials is that spin-orbit energies couple to higher-energy manifolds that preferentially suppress the spins perpendicular to the crystal-field easy axis.

---

[1] See, for example, K. Yosida, *Theory of Magnetism* (Springer, Berlin, 1996), Ch. 9.

[2] See, for example, H. T. Diep, *Frustrated Spin Systems* (World Scientific, Singapore, 2004).

[3] O. A. Starykh, A. V. Chubukov, and A. G. Abanov, Phys. Rev. B **74**, 180403(R) (2006); W. Zheng, J. O. Fjærestad, R. R. P. Singh, R. H. McKenzie, and R. Coldea, *ibid.* **74**, 224420 (2006); A. L. Chernyshev and M. E. Zhitomirsky, Phys. Rev. Lett. **97**, 207202 (2006).

[4] G. Lautenschläger, H. Weitzel, T. Vogt, R. Hock, A. Böhm, M. Bonnet, and H. Fuess, Phys. Rev. B **48**, 6087 (1993).

[5] M. Kenzelmann, A. B. Harris, S. Jonas, C. Broholm, J. Schefer, S. B. Kim, C. L. Zhang, S.-W. Cheong, O. P. Vajk, and J. W. Lynn, Phys. Rev. Lett. **95**, 087206 (2005).

[6] T. Arima, A. Tokunaga, T. Goto, H. Kimura, Y. Noda, and Y. Tokura, Phys. Rev. Lett. **96**, 097202 (2006).

[7] T. Nakajima *et al.*, Phys. Rev. B **79**, 214423 (2009).

[8] J. T. Haraldsen, F. Ye, R. S. Fishman, J. A. Fernandez-Baca, Y. Yamaguchi, K. Kimura, and T. Kimura, Phys. Rev. B **82**, 020404 (2010).

[9] M. Poienar, F. Damay, C. Martin, V. Hardy, A. Maignan, and G. André, Phys. Rev. B **79**, 014412 (2009); M. Poienar, F. Damay, C. Martin, J. Robert, and S. Petit, *ibid.* **81**, 104411 (2010).

[10] M. Frontzek, G. Ehlers, A. Podlesnyak, H. Cao, M. Matsuda, O. Zaharko, N. Aliouane, and S. Barilo (unpublished); M. Frontzek, J. T. Haraldsen, A. Podlesnyak, M. Matsuda, A. Christianson, R. S. Fishman, Y. Qiu, J. Copley, S. Barilo, S. V. Shiryaev, and G. Ehlers (unpublished).

[11] R. S. Fishman (unpublished).

[12] M. Hasegawa, M. I. Batrashevich, T. R. Zhao, H. Takei, and T. Goto, Phys. Rev. B **63**, 184437 (2001).

[13] T. Takagi and M. Mekata, J. Phys. Soc. Jpn. **64**, 4609 (1995).

[14] M. Swanson, J. T. Haraldsen, and R. S. Fishman, Phys. Rev. B **79**, 184413 (2009); J. T. Haraldsen, M. Swanson, G. Alvarez, and R. S. Fishman, Phys. Rev. Lett. **102**, 237204 (2009).

[15] S. Miyashita, J. Phys. Soc. Jpn. **55**, 3605 (1986).

[16] For instance, the magnetic field produces the order S term $\mathcal{H}_2' = 2\mu_B H \sum_{\mathbf{k},r} \cos\theta_r a_{\mathbf{k}}^{(r)\dagger} a_{\mathbf{k}}^{(r)}$. When $\mathcal{H}_2'$ is symmetrized as $\mu_B H \sum_{\mathbf{k},r} \cos\theta_r \{a_{\mathbf{k}}^{(r)\dagger} a_{\mathbf{k}}^{(r)} + a_{-\mathbf{k}}^{(r)} a_{-\mathbf{k}}^{(r)\dagger}\} - (\mu_B H N/3) \sum_r \cos\theta_r$, the first term satisfies the form $S \sum_{\mathbf{k}} \mathbf{u}(\mathbf{k})^\dagger \cdot \underline{L}(\mathbf{k}) \cdot \mathbf{u}(\mathbf{k})$ and the last term contributes to $S R_2$.

[17] M. A. van der Vegte, Ph.D. thesis, University of Groningen, 2010; M. A. van der Vegte, S. Artyukhin, and M. Mostovoy (unpublished).

[18] QFs do not change the average value M_{av} for a collinear state because a collinear state is an eigenstate of $S_{\text{tot},z} = \sum_i S_{iz}$ in the absence of QFs and $[S_{\text{tot},z}, \mathcal{H}] = 0$.

[19] A. V. Chubukov and D. I. Golosov, J. Phys. Condens. Matter **3**, 69 (1991).